Z Boson Detection in PP Collisions

Ian Ulrich*
Department of Physics, University of California, Los Angeles, Los Angeles, California 90024
(Dated: March 15, 2021)

I. INTRODUCTION

The overarching goal of High Energy Physics experiments is to better understand the constituents that make up the world around us as well as the fundamental interactions that dictate the behavior of those constituents. In this report we present evidence for the detection of one of the particles that has its foot in both doors, being a fundamental particle as well as playing a role in dictating the behavior of other particles, the Z boson. This is because the Z^0 is a real particle as well as a force mediator of the weak interaction, similar to the role the photon plays in electromagnetism. The Z^0 was first theorized by Glashow, Salam, and Weinberg in the late 1960's[1] and later was directly observed in the UA1 experiment at CERN in 1983 and was "greeted with jubilation as it confirmed the electroweak theory, a cornerstone of the Standard Model of particle physics developed during the 1970s"[2]. Here we will utilize a similar process as the UA1 experiment but will be dealing with PP collisions that will produce Z^0 through a process shown in Fig. 1.

II. CMS DETECTOR

The collision data that we will analyze comes from the Compact Muon Solenoid (CMS), a general purpose detector at the Large Hadron Collider (LHC). It gets its name from the fact that, for its size and the amount of materials inside it is relatively compact, can detected muons at a high precision and contains the strongest magnetic solenoid ever built[3]. The components of the CMS detector can be seen in Fig.2 (taken from CERN[3]). The detector is submerged in a 3.8T magnetic field made possible through the use of cylindrical coils of superconducting cable running an 18.5 kA current. The innermost component of the detector is a collection of silicon trackers that is able to accurately track particles produced in the collisions. The silicon trackers can be thought of as p-n junctions which have a depletion layer in the middle, and when high energy particles pass through these junctions they deposit enough energy to create an electron-hole pair. Due to the built up electric field in the p-n junctions, the electron and hole will be pulled to opposite sides of the p-n junction causing a small current in the tracker. We can gain a strong understanding of how the particles moved through the trackers by which trackers yielded current spikes. This is useful as it can tell us both the charge as well as the momentum of the particles that traverse the tracker (stronger curvature for lower momentum; direction of curvature for polarity of charge).
The detector is also the host to a hadronic calorimeter (HCAL) inside which hadronic particles (those made of quarks) may be detected. The HCAL is able to detect quarks in a similar manner as the ECAL which will be explained in detail below.

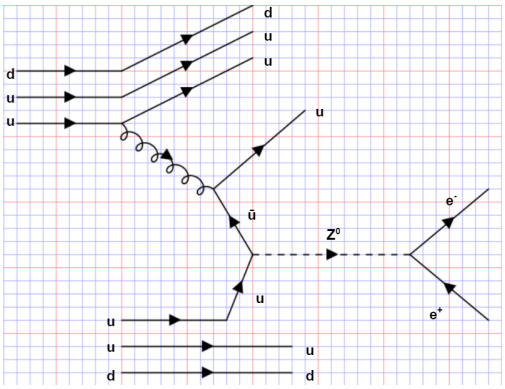

FIG. 1. $PP \rightarrow Z^0$ Feynman Diagram

A. Electromagnetic Calorimeter

However our main focus will be the electromagnetic calorimeter (ECAL) as it will allow us to measure the e^+e^- produced in the decay of the Z^0. This section of the detector is composed of over 75,000 lead tungstate ($PbWO_4$) crystals fitted with photodiodes at the ends. This is because charged particles moving through materials will emit radiation. At low energies(1 MeV) ionization is the dominant means of EM radiation but we expect an electron emitted in the decay of a Z^0 to have energy near 45 GeV. At this energy the dominant means of radiation is Bremsstrahlung where the electron will interact with a nuclei in the material emitting a virtual photon to the nuclei as well as a real photon, losing energy in the process. The photons produced in this process will be detected by the photodiode at the end of the $PbWO_4$ crystal. The energy a charged particle has after moving a given distance through a material while undergoing Bremsstrahlung is given by,

$$E = E_0 e^{-X/X_0} \tag{1}$$

* Ianulrich25@g.ucla.edu

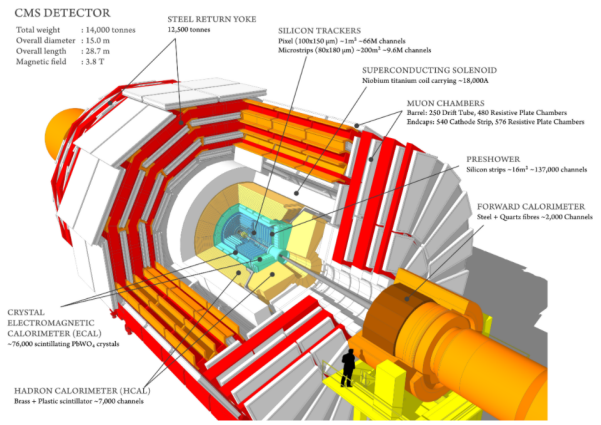

FIG. 2. CMS Section Diagram

where X is the distance traversed and X_0 is known as the radiation length, which is a property of a material. The radiation length of $PbWO_4$ is approximately 0.9cm making it an excellent candidate for the ECAL, as we need it to bring the electron to a stop in a reasonable amount of space. The $PbWO_4$ crystals in the CMS are cut to be 22cm in length to effectively diminish all energy in the electron.

$$E = 45GeVe^{-22cm/0.9cm} \approx 1eV \tag{2}$$

The face of the crystals are cut to be 2.2cm x 2.2cm because of a characteristic of materials known as the Moliere Radius. The Moliere Radius is the radius of a cylinder that would contain 90% of the EM shower radiation and can be determined by the Eq.3, where X_0 is again the radiation length and E_C is the critical energy of the material.

$$R_m = X_0\frac{91MeV}{E_c} = 0.9cm\frac{21MeV}{9MeV} \approx 2.2cm \tag{3}$$

The crystals are cut so that any given EM shower will cause signals in a minimum of 4 crystals. This is useful in two ways, first by observing the amount of the shower that is present in each of the crystals we can more accurately distinguish where the electron initially collided with the ECAL rather than the entire shower taking place in a single crystal. Secondly by allowing for multiple crystals to detect a single electron we can effectively reduce any electrical noise that might be present in our detectors. For example, if a single crystal detects some radiation but the surrounding crystals don't then we can omit this radiation as electrical noise.

III. ELECTRON IDENTIFICATION AND OPTIMISATION IN SIMULATION

We utilized simulation data of the Drell-Yan process(Fig. 1) as well as simulated random quantum chromodynamics(QCD) events to filter out any electrons that aren't produced through the decay of the Z^0 that could otherwise have skewed our data. This was done by performing cuts on important variables such that the electrons that shared characteristics with those of the Drell-Yan data set would make it through to Z^0 reconstruction while those that did not match those characteristics would be omitted. In analyzing these data sets we accessed collision data by using the CMS Gsfelectron variables ***energy, px, py, pz, pt, hcaloverecal, phi, eta, sigmaIetaIeta, dr03TkSumPt, dr03EcalRecHitSumEt,*** and ***dr03HcalTowerSumEt***. Before performing any analysis of the variables, we first performed a selection process where all suspected electrons in the Drell-Yan data set had to match to an initial e^-e^+ pair produced in a Monte Carlo simulation. This was done by creating a cone of radius 0.3 around all of the e^- and e^+ from the MC simulation and checking if any of the suspected electrons fell inside the cone. To determine if a suspected electron was inside a given cone, Eq. 4 was used, where $\delta\phi$ is the difference in the ϕ component of the suspected electron and the MC simulated electron and $\delta\eta$ is the difference in the *eta* component of the two(ϕ is a measure of the azimuthal angle a particle makes after collision and η, also known as the pseudorapidity, is a measure of the angle a particle taken with respect to the P beam and is given by Eq.5 where θ is the true angle). Any suspected electron that wasn't matched to a MC simulated electron was omitted from the data set.

$$\Delta R = \sqrt{\delta\phi^2 + \delta\eta^2} \tag{4}$$

$$\eta = -ln[\tan\frac{\theta}{2}] \tag{5}$$

The two dominant processes that we focused on filtering out was heavy flavor decay as well as $\pi^0 \to \gamma\gamma$ production each of which will produce unwanted electron signatures.

A. $\pi^0 \to \gamma\gamma$ Decay

The more dominant of the two processes is $\pi^0 \to \gamma\gamma$ (seen in Fig. 3) as it is mediated solely through the strong interaction which has the strongest coupling of all the fundamental interactions. In this process the π^0 is extremely unstable($\tau \approx 10^{-7}s$) and almost immediately decays into two photon that deposit their energy into the ECAL. This energy deposit along with the tracking of nearby quarks in the silicon trackers is so similar to that of a real electron that it will be included as an electron. The key difference we utilized is in the Z^0 decay, the e^- produced will deposit its energy into the ECAL with very little energy being deposited while the γ γ pair will be surrounded by quarks that will deposit their energies into the HCAL. (ideally the HCAL energy will be zero

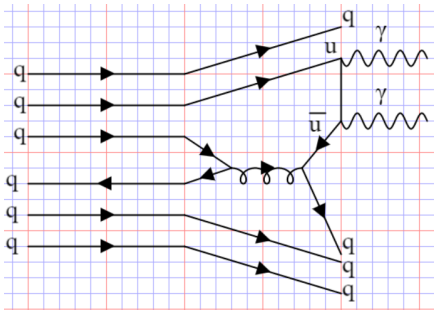

FIG. 3. Possible $\pi^0 \rightarrow \gamma\gamma$ Process

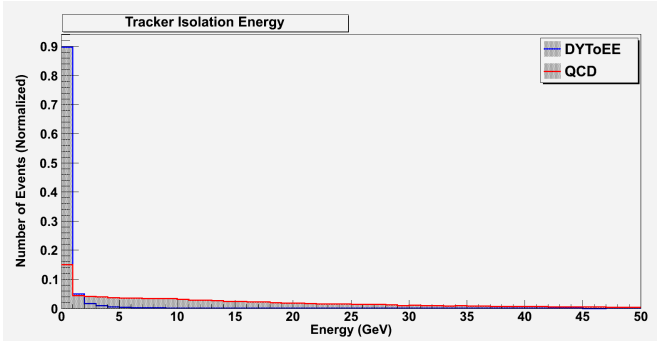

FIG. 4. Sum of Energy Deposit in Silicon Trackers

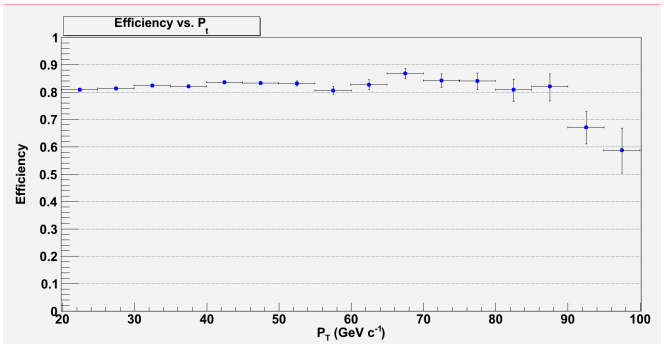

FIG. 5. Tight Fit Efficiency vs. P_T

in this case but for reasons stated in Sec. II we still have some readings for HCAL). Therefore we were able to use the variable *hcaloverecal* to distinguish between e^- signatures produced through Z^0 decay and those produced through π^0 decay.

B. Heavy Flavor Decay

Heavy flavor decay is when quarks in the collision annihilate via the strong force and produce two new quarks. Due to color confinement these quarks must form colorless states by radiating gluons that can produce quark pairs creating a hadronic shower. In this hadronic shower a quark can radiate a $W^{\pm}$, producing an $e^{\pm}\nu_e/\bar{\nu_e}$. *HCAL/ECAL* isn't sufficient in distinguishing this electron from the good electrons as this electron will be found away from the hadronic shower that produced it cause a reasonably low *HCAL/ECAL* value. However we can utilize the isolation variables *dr03TkSumPt, dr03EcalRecHitSumEt*, and *dr03HcalTowerSumEt* to distinguish these electrons from the good ones. These variables create a cone around the suspected electron and take the sum of all of the energy deposited into the silicon trackers, the ECAL, and the HCAL. While the *HCAL/ECAL* wasn't able to capture the hadronic behavior near the suspected electron, these variables are able to see the extra energy deposits throughout the detector. For an electron created in the Z^0 decay these values are expected to be very low.

C. Cuts

Knowing the expected behavior of the variables discussed, we were able to look at them individually and compare the values of the electrons from the Drell-Yan set that were matched to the MC simulation and electrons in the random QCD set and determine cuts. A histogram of the total energy deposited into the trackers used to distinguish between true electrons and heavy flavor decay (Fig. 4). Here we can see that a cut at dr03TkSumPt <1GeV will effectively omit roughly 80% of the QCD events while still keeping roughly 90% of the Drell-Yan data. This process was repeated to determine cuts for the variables *hcaloverecal, dr03TkSumPt, dr03EcalRecHitSumEt, dr03HcalTowerSumEt*, and *sigmaIetaIeta*, the last of which is simply a measure of spread in clusters of energy deposits in the detector.

D. Efficiency and Fake Rate

In order to measure the quality of our cuts we performed efficiency and fake rate analysis. The efficiency of the cuts is a measure of how many of the true e^-e^+ from the Drell-Yan data set made it past the cuts implemented and the fake rate of the cuts is a measure of how many of the random QCD events made it past the cuts. Two efficiencies were generated when determining the cuts, a tight fit of 80% efficiency and a loose fit of 90% efficiency. When analyzing real PP collisions to detect the Z^0 the tight fit cuts were used. The tight fit efficiency and fake rate can be seen in Fig. 5 and Fig. 6.

IV. RECONSTRUCTION OF DI-ELECTRIC INVARIANT MASS

At this point we have effectively applied cuts so that only e^-e^+ that come from the Z^0 decay would be present in the real PP collision data set and all that is left is

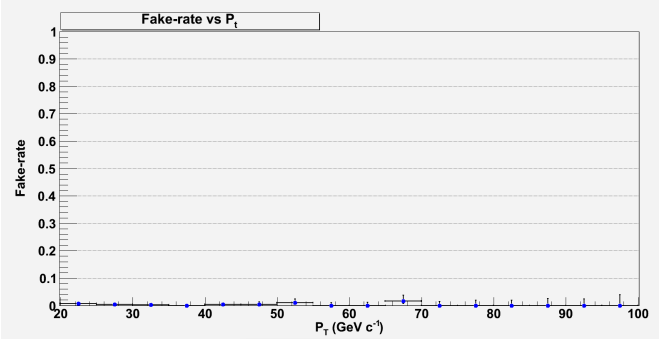

FIG. 6. Tight Fit Fake Rate vs. P_T

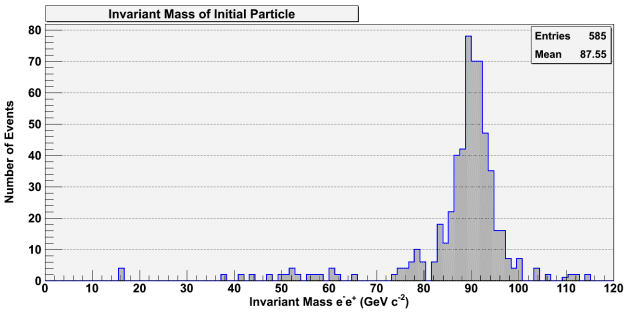

FIG. 7. Invariant Mass for PP Collision After Cuts

reconstructing the invariant mass of the Z^0. In events where there weren't two or more electrons identified we omitted the entire event. In the events where more than two electrons made it through the cuts we reconstructed the invariant mass using the most energetic electrons. We expect the energy of e^-e^+ to be nearly 45GeV as both would take half of the energy of the Z^0. At this energy the mass of electron is negligible and we can write the energy in standard units as,

$$E_{e^-}^2 = c^4m^2 + c^2p^2 = m^2 + p^2 \approx p_{e^-}^2 \tag{6}$$

First we add the two four vectors,

$$p_{e^-} + p_{e^+} = (E_{e^-} + E_{e^+}, \vec{p_{e^-}} + \vec{p_{e^-}}) \tag{7}$$

To get the invariant mass we take the square of the sum of the two four vectors,

$$p_{Z^0}^2 = m_{Z^0}^2 + p_{Z^0}^2 = m_{Z^0}^2 = E_{e^-}^2 - p_{e^-}^2 + E_{e^+}^2 - p_{e^+}^2 + 2\vec{p_{e^-}} \vec{p_{e^+}} \tag{8}$$

Taking $E_{e^\pm} \approx p_{e^\pm}$ we are left with,

$$m_{Z^0}^2 = 2\vec{p_{e^-}} \cdot \vec{p_{e^+}} \tag{9}$$

Which can be written as,

$$m_{Z^0} = \sqrt{2E_{e^-}E_{e^+} - p_{e^-x}p_{e^+x} - p_{e^-y}p_{e^+y} - p_{e^-z}p_{e^+z}} \tag{10}$$

With Eq.10 we were able to calculate the invariant mass of the $e^{-\prime}s$ $e^{+\prime}s$ in a data set of real PP collisions and obtained values for m_{Z^0} shown in Fig.7. Our data agrees with the accepted mass of the Z^0 coming within 4 $GeVc^{-2}$.

[1] The nobel prize in physics 1979. https://www.nobelprize.org/prizes/physics/1979/summary/. Accessed: 2021-03-14.

[2] Izlar, Kelly. Thirty years of the z boson. https://home.cern/news/news/physics/thirty-years-z-boson. Accessed: 2021-03-14.

[3] CERN. Cern accelerating science. https://cms.cern/detector. Accessed: 2021-03-14.